The role of flexoelectricity in pattern formation

Ágnes Buka[1], Tibor Tóth-Katona[1], Nándor Éber[1],
Alexei Krekhov[2], and Werner Pesch[2]

[1]*Research Institute for Solid State Physics and Optics, Hungarian
Academy of Sciences, H-1525 Budapest, P.O.B. 49, Hungary
e-mail: ab@szfki.hu, katona@szfki.hu, eber@szfki.hu*

[2] *Physikalisches Institut, Universität Bayreuth, D-95440 Bayreuth,
Germany
e-mail: alexei.krekhov@uni-bayreuth.de, werner.pesch@uni-bayreuth.de*

In this chapter the influence of flexoelectricity on pattern formation induced by an electric field in nematics will be summarized. Two types of patterns will be discussed in the linear regime, the equilibrium structure of flexoelectric domains and the dissipative electroconvection (EC) rolls. In a separate section, recent experimental and theoretical results on the competition and crossover between the flexoelectric domains and EC patterns will be described.

Contents

4.1. Introduction

Patterns, i.e. regular spatio-temporal structures, can easily be generated in liquid crystals via a large variety of external stresses, e.g., by mechanical shear, temperature or pressure gradients, electric or magnetic fields,

etc.; representative examples are found in Ref. 1. Here we concentrate on patterns induced by electric fields in nematics and in particular on the implications of flexoelectricity.

Nematics are uniaxial fluids; the preferred axis is defined by a unit vector $\boldsymbol{n}$, the director.[2] We consider a thin nematic layer of thickness d confined between two plates (parallel to the x, y-plane), which impose the initial direction $\boldsymbol{n}_0$ of $\boldsymbol{n}$ in the basic state. The plates also serve as electrodes for the application of an electric field $\boldsymbol{E}$ along the z-axis.

As a consequence of the uniaxial symmetry all material properties of nematics have to be represented by tensors. For instance, the dielectric displacement $\boldsymbol{D}$ and $\boldsymbol{E}$ are connected by the dielectric susceptibility tensor $\boldsymbol{\epsilon}$ as $\boldsymbol{D} = \epsilon_0 \boldsymbol{\epsilon} \boldsymbol{E} \equiv \epsilon_0 [\epsilon_\perp \boldsymbol{E} + (\epsilon_\parallel - \epsilon_\perp)(\boldsymbol{n} \cdot \boldsymbol{E})\boldsymbol{n}]$. Thus $\boldsymbol{\epsilon}$ depends in general on the local director orientation and is specified by the two dielectric constants, $\epsilon_\parallel$ and $\epsilon_\perp$ (for $\boldsymbol{E}$ parallel and perpendicular to $\boldsymbol{n}$, respectively). An analogous representation applies to the electric conductivity tensor $\boldsymbol{\sigma}$.

Any spatial distortion of $\boldsymbol{n}$ leads to elastic restoring torques, which are determined in the standard continuum description of nematics (exclusively used in this review) by the three elastic constants K_1 (splay), K_2 (twist), and K_3 (bend).[2] In addition, the electric field $\boldsymbol{E}$ gives rise to an electric torque on the director. The balance of these torques, reflected in the resulting equilibrium director configuration, corresponds to the minimum of the orientational free energy $\mathcal{F}(\boldsymbol{n})$. In the case of positive dielectric anisotropy ($\epsilon_a = \epsilon_\parallel - \epsilon_\perp$) the dielectric torque ($\propto |\boldsymbol{E}|^2$) is destabilizing in the planar director configuration ($\boldsymbol{n}_0 \parallel \boldsymbol{x}$). With increasing $|\boldsymbol{E}|$ above a certain threshold E_F the electric torque becomes obviously larger than the stabilizing elastic torque (determined by the elastic constants). Thus an initial planar director configuration will experience a splay distortion in the form of an out-of-plane rotation of $\boldsymbol{n}$. This process, the *Freedericksz transition*,[2] is a prominent example of an orientational transition in nematics under the influence of an applied electric field. Since $\mathcal{F}(\boldsymbol{n})$ of the distorted state becomes lower than that of the basic state at E_F, the notion of an *equilibrium phase transition* is common in analogy to standard thermodynamics.

In most cases the stationary director configuration resulting from the Freedericksz transition in planar geometry is uniform in the plane of the layer and varies only in the z-direction. However, in some exceptional cases, when the splay elastic constant K_1 is much larger than the twist elastic constant K_2 (e.g., in liquid crystal polymers), a spatially periodic out-of-plane director distortion becomes energetically favourable. The resulting splay-twist (ST) Freedericksz state is manifested in the experiments in the form

of a "longitudinal" stripe pattern,[3] running parallel to the initial director alignment $\boldsymbol{n}_0 \parallel \boldsymbol{x}$.

Besides the elastic and the electric torques the so called *flexoelectric* (or *flexo*) torques on the director play an important role as well. Their impact on pattern forming instabilities in nematics is the main issue of the present review. Flexo torques originate from the fact that typically (in some loose analogy to piezoelectricity) any director distortion is accompanied by an electric "flexo" polarization $\boldsymbol{P}_{\text{fl}}$ (characterized by the two flexocoefficients e_1, e_3).[2,4] From a microscopic point of view finite e_1, e_3 naturally arise, when the nematic molecules have a permanent dipole moment.[4] But also in the case of molecules with a quadrupolar moment finite e_1, e_3 are possible[5] (see also Chapter 1 in this book[6]). The flexo polarization has to be incorporated into the free energy $\mathcal{F}(\boldsymbol{n})$ for finite $\boldsymbol{E}$. It is not surprising that this leads to quantitative modifications of phenomena already existing for $e_1 = e_3 = 0$. Though, for example, the Freedericksz threshold field E_F is not modified, the presence of flexoelectricity leads to considerable modifications of the Freedericksz distorted state for $|\boldsymbol{E}| > E_F$.[7]

Much more exciting is the possibility of qualitatively new phenomena, which are generically related to the flexo polarization. A prominent example is provided by the so called flexo-domains. They appear as the result of an equilibrium transition from the basic planar state if the applied electric field strength exceeds a certain threshold, E_{fl}. Flexo-domains are stripe patterns parallel to the imposed preferred direction $\boldsymbol{n}_0 \parallel \boldsymbol{x}$, i.e. with a wave vector $\boldsymbol{q}_c \perp \boldsymbol{x}$.[8–12] In contrast to the standard Freedericksz transition, the sign of ϵ_a plays no role, but the difference $|e_1 - e_3|$ has to be large enough.

More frequently than the equilibrium pattern sketched so far, one observes electroconvection (EC) patterns in nematics, which present dissipative structures characterized by director distortions, space charges and material flow. A necessary requirement for their existence is the presence of charge carriers in the nematic. In a distorted nematic, where $\boldsymbol{n}$ is neither parallel nor perpendicular to $\boldsymbol{E}$, the generation of a nonzero space charge, ρ_{el}, by charge separation is then inevitable. The resulting Coulomb force in the flow equations (generalized Navier-Stokes equations) drives a flow which in turn exerts a destabilizing *viscous torque* on the director. Under favourable conditions stabilizing elastic and electric torques may be overcompensated leading to a *non-equilibrium phase transition* from the basic quiescent state. As a result a periodic array of convection rolls appears if the strength of $\boldsymbol{E}$ is above the EC threshold.[13–16] To understand the majority of EC convection patterns investigated in the past it has been suffi-

cient to analyze the *standard* nemato-electrohydrodynamic model,[15] where flexoelectricity is not included. More recently a specific class of nematic materials has been studied,[17,18] where the interpretation of the observed EC patterns ("nonstandard EC") definitively requires the inclusion of flexoelectricity into the theoretical description.[19]

Patterns in nematics are easily observed by optical means, where the anisotropy of the refractive index is exploited. In this way the stripe patterns in electroconvection in the planar geometry are easily discriminated from flexo-domains: the angle α between the wave vector $\boldsymbol{q}$ of the EC stripes and the preferred direction $\boldsymbol{n}_0 \parallel \boldsymbol{x}$ is small (normal or oblique rolls), in contrast to $\alpha = 90°$ (longitudinal stripes) in flexo-domains.

In the following we will exclusively concentrate on the final states, which are reached by the system in an applied field when all transients have died out. To resolve these transients in experiments and to analyze them in theory is a highly demanding task, but certainly gives important additional insights. For instance in the development of the homogeneous splay Freedericksz state one observes two kinds of *transient patterns*.[21] For nematics with small (positive) ϵ_a the stripes are oriented almost perpendicular to the initial director alignment $\boldsymbol{n}_0$ ($\alpha \approx 0$) while for large ϵ_a the stripes are parallel to $\boldsymbol{n}_0$ ($\alpha \approx 90°$). In these stripe patterns flow is present until the final equilibrium structure is established; thus the theoretical analysis has to be based on the full electrohydrodynamic equations. The stripes perpendicular to $\boldsymbol{n}_0$ have been explained in the framework of a linear stability analysis of the basic planar state.[21] The appearance of parallel stripes has been captured by a non-linear analysis taking into account the time evolution of the Freedericksz state.[20] Here the effect of field inhomogeneity due to the large ϵ_a plays an important role, that favours stripes parallel to $\boldsymbol{n}_0$. Another example of transients is the decay of an EC pattern when turning off the applied electric field.[22,23] In these cases one has indeed obtained deeper insights into the complex interplay of the various mechanisms responsible for patterns in nematics, which also opens additional routes to determine some material parameters. As far as we know, the effect of flexoelectricity has not yet been studied for these transient patterns. It would be certainly rewarding to study other situations where flexoelectricity might become more important during the transients than in the final state.

In this review we focus in particular on recent theoretical and experimental investigations in the planar geometry, which are mostly restricted to the linear regime, i.e. to applied electric field strengths $|\boldsymbol{E}|$ slightly above the respective threshold fields. We put some emphasis on the rather unique

aspect of nematics, that they allow to study in the same experimental setup the competition between the (equilibrium) flexo-domains, and the dissipative EC patterns by changing the circular frequency ω of the applied AC electric field.

The review is organized as follows: Sec. 4.2 is devoted to the flexo-domains in the planar geometry. Particular emphasis is put on most recent theoretical results, where for the first time arbitrary ratios of the elastic constants K_1, K_2 are considered as well as the driving by an AC electric field. Section 4.3 deals with the impact of the flexoelectricity on the dissipative EC patterns. Focus is in particular on qualitatively new phenomena which are not covered by the standard model of EC. Then in the following Sec. 4.4 we analyse the competition between flexo-domains and EC patterns at low AC driving frequencies. The review will be completed by a discussion and some concluding remarks in Sec. 4.5.

4.2. Equilibrium structures: flexo-domains

As already noted in the introduction, the flexo torques in the presence of an electric field in nematics can lead to spatially periodic, equilibrium director distortions, the flexo-domains. The characteristic static, "longitudinal stripes" of flexo-domains oriented parallel to $\boldsymbol{n}_0 \parallel \boldsymbol{x}$ have been first observed more than 40 years ago under the action of a DC electric field[8,9] in the planar geometry (for an example, see Fig. 4.1). As first described in the work of Bobylev and Pikin,[10] *flexoelectricity* indeed provides a natural mechanism (independent of the sign of ϵ_a) to explain these stripes. Here the well known fact has been exploited that splay and/or bend director distortions are generically associated with the flexo polarization

$$\boldsymbol{P}_{\mathrm{fl}} = e_1 \boldsymbol{n}(\nabla \cdot \boldsymbol{n}) + e_3 (\boldsymbol{n} \cdot \nabla) \boldsymbol{n} \ , \tag{4.1}$$

where e_1, e_3 are the splay and bend flexoelectric coefficients, respectively.[4] Thus in the presence of an electric field $\boldsymbol{E}$ the free energy density of nematics contains, in addition to the elastic and electric contributions, the flexo term

$$\mathcal{F}_{\mathrm{fl}} = -\boldsymbol{P}_{\mathrm{fl}} \cdot \boldsymbol{E} \ , \tag{4.2}$$

which results in the flexoelectric torque $\boldsymbol{n} \times (\delta \mathcal{F}_{\mathrm{fl}}/\delta \boldsymbol{n})$. It turns out that the flexoelectric torque depends only on the difference $(e_1 - e_3)$ and favours, as will be shown below, flexo-domains for sufficiently large $|e_1 - e_3|$ if the strength of $\boldsymbol{E}$ is above a certain threshold $|\boldsymbol{E}| = E_{\mathrm{fl}}$.
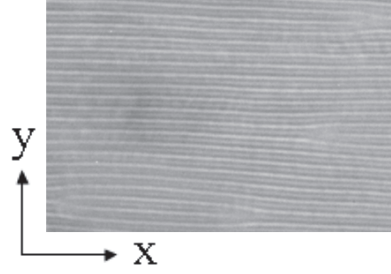
Fig. 4.1.   Snapshot of the flexo-domains in a planar nematic **Phase 4** with the preferred axis parallel to $\boldsymbol{n}_0 \parallel \boldsymbol{x}$.

The theoretical analysis of flexo-domains in planar nematics, which is briefly reviewed in the following, exploits the balance of torques by minimizing the total free energy $\mathcal{F}(\boldsymbol{n})$. If not otherwise stated, the assumption of a *strong anchoring* of the director $\boldsymbol{n}$ at the confining plates is used; i.e. the director at the boundaries remains parallel to $\boldsymbol{n}_0 \parallel \boldsymbol{x}$, irrespective of director distortions in the bulk of the nematic layer.

Let us start with the case of DC driving. In the one-elastic-constant approximation (*isotropic elasticity*, i.e. $K_1 = K_2 = K_3 = K_{av}$) the director equations originating from the torque balance can be solved analytically in the linear regime of small distortions of the planar basic state. One arrives at a closed threshold formula for the critical voltage $U_c = E_{fl}d$ and the critical wave number q_c of the longitudinal rolls:[10,11,24,25]

$$U_c = \frac{2\pi K_{av}}{|e_1 - e_3|(1 + \mu)} \ , \quad q_c = \frac{\pi}{d}\left(\frac{1 - \mu}{1 + \mu}\right)^{1/2} \ , \tag{4.3}$$

where

$$\mu = \frac{\epsilon_0 \epsilon_a K_{av}}{(e_1 - e_3)^2} \ . \tag{4.4}$$

According to Eq. (4.3) the flexo-domains exist only (q_c has to be finite!) if $|\mu| < 1$, i.e.,

$$|\epsilon_a| < \frac{(e_1 - e_3)^2}{\epsilon_0 K_{av}} \ . \tag{4.5}$$

As a function of μ both U_c and q_c rise monotonically from $\mu = 1$ on until they diverge in the limit $\mu \to -1$.

The distortions of the basic director orientation $\boldsymbol{n}_0 \parallel \boldsymbol{x}$ in the flexo-domains are characterized by an out-of-plane component ($n_z \neq 0$) and

an in-plane rotation ($n_y \neq 0$), which are periodic in the $y-$direction and depend on z.

The analysis of flexo-domains in the general case of anisotropic orientational elasticity ($K_1 \neq K_2$) is in principle straightforward.[26] One arrives quite easily at a transcendental equation for the "neutral curve" $U_0(q)$ (first given in Ref. 24) at which the bifurcation of flexo-domains with wave number q from the basic planar state takes place. Solving numerically for $U_0(q)$ and subsequently minimizing $U_0(q)$ with respect to q yields the critical wave number q_c and the critical voltage $U_c \equiv U_0(q_c)$.

One of the central results of the analysis in the case of anisotropic elasticity at DC voltage driving is presented in Fig. 4.2. It shows the range of existence of the flexo-domains (marked as the grey region) in the $(\mu, \delta k)$ plane, where μ has been defined in Eq. (4.4). The elastic constants K_1, K_2 have been parameterized in terms of the average value $K_{av} = (K_1 + K_2)/2$ of the elastic constants, and by the relative deviation δk from K_{av} in the following manner:

$$K_1 = K_{av}(1 + \delta k) , \quad K_2 = K_{av}(1 - \delta k) . \tag{4.6}$$

Obviously $|\delta k| < 1$ is required. The case $\delta k > 0$ (i.e., $K_2 < K_1$) corresponds to rod-like nematics like **MBBA** (N-(4-metoxybenzylidene)-4-butylaniline), while $\delta k < 0$ (i.e., $K_2 > K_1$) holds for discotic nematics.

The $(\mu, \delta k)$ range of flexo-domains is limited from above by the upper limiting curve, $\mu_{max}(\delta k) > 0$ (dashed line in Fig. 4.2). At larger μ, e.g. at larger ϵ_a, the homogeneous Freedericksz state takes over. Note that $\mu_{max}(\delta k)$ diverges at $\delta k \approx 0.53$. This divergence is closely related to the existence of the spatially periodic splay-twist (ST) Freedericksz stripes for $\delta k \gtrsim 0.53$ in the absence of the flexo torque ($e_1 - e_3 = 0$) for $\epsilon_a > 0$.[3,27,28] Actually, the ST director state (known for more than two decades, and shown as ST in the upper right corner of Fig. 4.2) expands into the existence range of flexo-domains for nonzero flexoelectricity as has been discussed in more detail in Ref. 26.

On the other hand, the existence regime of flexo-domains is limited from below by the lower limit curve $\mu_{min}(\delta k) < 0$ (the solid line in Fig. 4.2). Since the electric torque is stabilizing for $\epsilon_a < 0$ ($\mu < 0$) in the planar geometry such a line must exist, at which the destabilization of the basic state by the flexo torque becomes impossible. Since with decreasing δk the relative strength of the flexo torque increases,[26] $\mu_{min}(\delta k)$ bends down leading to $\mu_{min}(\delta k) \to \infty$ for $\delta k \to -1$. Fig. 4.2 also demonstrates that in the one-elastic-constant approximation ($\delta k = 0$, $K_1 = K_2$) the limits

$\mu_{min}(0) = -1$, $\mu_{max}(0) = 1$ in Eq. (4.3) are recovered.
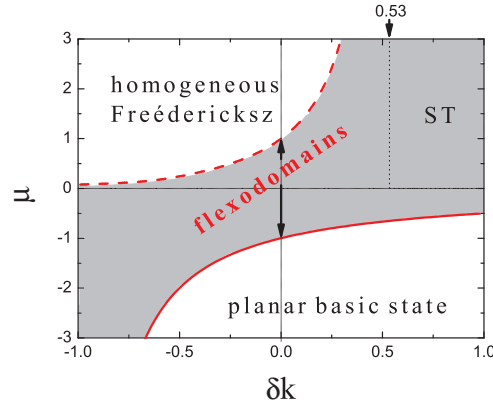

Fig. 4.2. Upper and lower limit curves, $\mu_{max}(\delta k)$ (dashed line) and $\mu_{min}(\delta k)$ (solid line), respectively, determining the range of existence of flexo-domains (grey region) in the $(\delta k, \mu)$ plane. The rectangular region marked as ST shows the range of existence of the spatially periodic splay-twist Freedericksz structure for $\delta k \gtrsim 0.53$, $e_1 - e_3 = 0$ and $\epsilon_a > 0$. The double arrow indicates in the one-elastic-constant approximation ($\delta k = 0$) the range of existence of flexo-domains ($|\mu| < 1$).

Rigourous closed expressions for U_c and q_c, as given in Eq. (4.3) for the special case $\delta k = 0$, do not exist for the general case of anisotropic orientational elasticity ($K_1 \neq K_2$). Some characteristic curves for typical material parameter sets of nematics are given in Ref. 26, to which we point for details. Qualitatively the U_c, q_c curves as function of μ look very similar to the ones in Eq. (4.3) for $\delta k = 0$, except that they are supported on a larger interval $\mu_{min}(\delta k) < \mu < \mu_{max}(\delta k)$. As long as $|\delta k| < 0.3$ and $|\mu| < 0.3$, the deviations of $U_c(\mu)$ and $q_c(\mu)$ from the values for $\delta k = 0$ [Eq. (4.5)] are quite small. This applies, for instance, to the nematic **Phase 4** where $\delta k = 0.21$ and $\mu = -0.3$, as follows from Ref. 29.

For completeness we would like to mention that a recent approximate numerical analysis[31] of the flexo-domains in the DC case taking into account anisotropic elasticity reproduces the general features of the rigourous calculations.[26] Note, however, that an analytical treatment of the problem[32,33] suffers from a methodological error as has been pointed out recently.[26,34] Therefore the expressions for U_c and q_c shown in[32,33] for $\delta k \neq 0$ are not

correct.

For an AC driving voltage flexo-domains have been analyzed as well by means of numerical solutions of the linear director (torque balance) equations.[26] In general, the existence of flexo-domains for a specific material parameter set in the DC case seems to be a necessary prerequisite for their existence when an AC voltage is applied. The analysis has been restricted to the low frequency range $\omega\tau_{\mathrm{d}} < 20$, which corresponds to frequencies $f = \omega/2\pi$ up to 20 Hz for a 10 μm thick **MBBA** layer.[26] (The director relaxation time τ_{d} is defined in the following section.) It seems to be needless to study flexo-domains for larger ω, since in all situations studied so far they are replaced either by the equilibrium Freedericksz state or by EC pattern.

The solutions of the linear equations for the director distortions $n_z(y, z, t)$, $n_y(y, z, t)$ are periodic in the $y-$direction as in the DC case, but depend explicitly on time as well. Since the linear equations are invariant against a time shift by half a period, $\mathcal{T}: t \to t + \pi/\omega$, we have two classes of solutions characterized by $\mathcal{T}n_z(t) = \mathfrak{p}n_z(t)$ with $\mathfrak{p} = \pm 1$. Which symmetry class is realized at the onset of flexo-domains depends on ω. The case $\mathfrak{p} = 1$ defines the solutions with the so-called "conductive symmetry", where the time average of n_z over one period is finite; the complementary case $\mathfrak{p} = -1$ corresponds to solutions with the "dielectric symmetry" where the time average of $n_z(t)$ vanishes. The time symmetry of the in-plane director component is opposite, i.e. $\mathcal{T}n_y(t) = -\mathfrak{p}n_y(t)$ holds.

As a consequence the limit $\omega \to 0$ is not smooth, since in the DC case ($\omega = 0$) the time average of both n_z and n_y are finite. A closer look at the director dynamics in the AC case shows that nonzero values of $n_z(t)$ and $n_y(t)$ appear only during a very small fraction of the period $T = 2\pi/\omega$. This means, that the patterns appear in the experiments only for very short time intervals as a flash. This phenomenon has indeed been observed in experiments to be discussed in Sec. 4.4.

The dependence of U_c and q_c of flexo-domains on the strength of the flexocoefficients, on the frequency ω, and on the elastic constants has been discussed in Ref. 26 as well. In general both U_c (see Fig. 4.5 below) and q_c rise very steeply as function of ω. Thus for $\mu > 0$ ($\epsilon_a > 0$) the bifurcation to the homogeneous Freedericksz state (with an $\omega-$independent critical voltage) will prevail already at very small ω. The competition with standard EC will be discussed in Sec. 4.4. In view of the discontinuities of $n_z(t)$ and $n_y(t)$ at $\omega \to 0$ discussed before it is not surprising that $U_c(\omega)$ and $q_c(\omega)$ are also discontinuous at $\omega \to 0$.[26] Note, that this has not been anticipated

in earlier investigations. As a caveat, however, it is worth mentioning that these discontinuities are much less expressed, when using a square waveform instead of a sinusoidal one.

There exists only one investigation of flexo-domains in the weakly non-linear regime for $U \gtrsim U_c$ in the DC case.[35] Based on a clever variational *ansatz* for the director distortion it has been demonstrated, that the director amplitudes grow continuously as $(U - U_c)^{1/2}$ (forward bifurcation). As a byproduct an approximate expression for the $\mu_{max}(\delta k)$ shown in Fig. 4.2 has been obtained.

So far we have restricted ourselves to strong anchoring of the director at the confining plates. The case of weak anchoring, where the director orientation at the plates is sensitive to the distortions in the bulk, has been considered as well[36,37] for $K_1 = K_2$. No qualitatively new scenarios, but only quantitative corrections of U_c and q_c have been predicted. These depend on two additional material parameters to describe the "surface potential" of the director, which in most cases have not been measured.

Experimental observations of the flexo-domains have been made in *planar geometry* for various nematics either with $\epsilon_a < 0$ (where the Freedericksz transition is excluded),[11,12,29,41,42] or with $\epsilon_a > 0$.[11,12,35,43] Precise comparison of the theory of flexo-domains with experiments requires at first a knowledge of the material parameters ϵ_a, K_1, K_2. These have been measured independently for some nematics like **MBBA**, **Phase 4**, **Phase 5**. However, since these parameters are typically not measured *in situ* (in the same cell), some scatter of their values in different experiments cannot be excluded: the compounds may come from different manufactures, could be contaminated, etc. The situation with the flexocoefficients is much more unsatisfactory (see, e.g. Chapter 2 in this book[44]). First of all their direct measurements are quite complicated and are thus rare. In addition the results of different measurements deviate substantially in almost all cases. Thus the flexocoefficients are often used as fitting parameters in the comparison of theory and experiments. We will postpone a more detailed discussion of the flexocoefficients to Sec. 4.5, after having discussed EC patterns and their possible competition with flexo-domains at low ω.

Flexo-domains have also been observed and analyzed in the twisted geometry (with a twist angle $\pi/2$) in **BMAOB** (p-n-butyl-p-methoxyazoxybenzene) in DC electric fields.[38] The flexo-domains are then oriented almost parallel to the initial director orientation in the midplane of the cell (i.e. at an angle of $\pi/4$). The threshold voltage was found to be slightly higher than for the planarly oriented sample. In addition the

instabilities for twist angles in the range $0 \ldots 5\pi/2$ have been studied by adding a small amount of a cholesteric compound to **BMAOB**. The onset characteristics of the flexo-domains in twisted geometry are well described by the theory.[38]

Flexoelectric patterns exist also for nematic layers with asymmetric boundary conditions, i.e. with homeotropic anchoring on one surface and planar anchoring on the other one (*hybrid aligned nematics* – HAN).[39,40] The critical voltage and the critical wave number obtained within the one-elastic-constant approximation are in a good agreement with the experimental results.[39]

Besides the flexo-domains, Hinov and his coworkers have promoted the existence of another flexoelectrically driven stripe pattern in nematics for which the notion *flexo-dielectric walls* has been coined.[45–47] Though these patterns, which have mostly been investigated in **MBBA** and also in **BMAOB**, are also oriented parallel to the preferred director alignment, they seem to differ substantially in other respects from the flexo-domains discussed above.[46] The flexo-dielectric walls have been observed under special boundary conditions, e.g. pretilt of the director, weak surface anchoring. A finite electrical conductivity and apparently a negative dielectric anisotropy of the nematics used in the experiments seems to be crucial. Moreover, it is reported that the flexo-dielectric walls are more concentrated near one of the electrodes depending on the polarity, in clear contrast to the standard flexo-domains residing in the bulk of the nematic layer. Since the experimental data are so far insufficient to clarify the origin of the flexo-dielectric walls and convincing theoretical models are still missing, flexo-dielectric walls will not be discussed in detail.

4.3. Dissipative structures: electroconvection

Electroconvection (EC) in nematics is certainly a prominent paradigm for non-equilibrium pattern forming instabilities in anisotropic systems. As already mentioned in the introduction, the viscous torques induced by a flow field are decisive, which is caused by an induced charge density, ρ_{el}, when the director varies in space. The electric properties of nematics with their quite low electric conductivity $[\sim 10^{-8} \ (\Omega \ \mathrm{m})^{-1}]$ are well described within the electric quasi-static approximation, i.e. by charge conservation and Poisson's law. Thus ρ_{el} is determined by the equations:

$$\frac{d}{dt}\rho_{el} + \nabla \cdot \boldsymbol{j}_{el} = 0 \ , \ \ \rho_{el} = \nabla \cdot (\epsilon_0 \boldsymbol{\epsilon} \boldsymbol{E} + \boldsymbol{P}_{\mathrm{fl}}) \ , \tag{4.7}$$

where the current density is given as $\boldsymbol{j}_{el} = \boldsymbol{\sigma}\boldsymbol{E}$. In analogy to $\boldsymbol{\epsilon}$ the electrical conductivity tensor $\boldsymbol{\sigma}$ is characterized by the two conductivities $\sigma_\parallel$, $\sigma_\perp$.

The physical phenomena involved in electroconvection are characterized by three different time scales, the director relaxation time $\tau_{\mathrm{d}} = \frac{\gamma_1 d^2}{K_1 \pi^2}$, the charge relaxation time $\tau_{\mathrm{q}} = \frac{\epsilon_0 \epsilon_\perp}{\sigma_\perp}$, and the viscous relaxation time $\tau_{\mathrm{v}} = \frac{\rho d^2}{\alpha_4/2}$. Here d is the layer thickness, ρ is the mass density, γ_1 is the rotational viscosity, and $\alpha_4/2$ is the isotropic viscosity. Typically $\tau_{\mathrm{d}} \gg \tau_{\mathrm{q}} \gg \tau_{\mathrm{v}}$,[16] such that the flow dynamics follows adiabatically the dynamics of the director and of the electric charges. As in most studies in this field, our focus is on the EC instability driven by a sinusoidal AC electric field, where the circular frequency $\omega = 2\pi f$ serves as an important control parameter besides the voltage amplitude. We will exclusively concentrate on anisotropic EC in the planar geometry, which has been discussed in a number of reviews in the last years (see, e.g. Refs. 1,16,48,49). According to the inseminating ideas of Carr and Helfrich the mechanism underlying EC becomes most transparent in the planar geometry when the electric anisotropies fulfil the conditions $\epsilon_a < 0$ and $\sigma_a = (\sigma_\parallel - \sigma_\perp) > 0$. In this case and for $\omega\tau_{\mathrm{d}} \gg 1$ the "standard model" without flexoelectricity is sufficient to understand the main features of EC. The roll patterns are usually oriented perpendicular [normal rolls, Fig. 4.3(a)], or nearly perpendicular [oblique rolls, Fig. 4.3(b)] to the preferred direction $\boldsymbol{n}_0 \parallel \boldsymbol{x}$. The latter appear usually at low frequencies below the so called Lifshitz frequency ω_L and are replaced by the normal rolls above ω_L. Oblique rolls come in two symmetry degenerate species: *zig* and *zag*. They appear either in separated patches as in Fig. 4.3(b) or superimposed leading to rhomboidal grid patterns[50] (not shown here). In analogy to the flexo-domains, we find EC pattern both with the conductive temporal symmetry (finite time average of n_z) and with dielectric symmetry (zero time average of n_z). The conductive symmetry is observed at ω below a cut-off frequency, ω_c, above which the dielectric symmetry prevails at onset.

Regarding the impact of flexoelectricity, the first theoretical investigations have basically focused on the conductive regime[51,52] in planar electroconvection for $\epsilon_a < 0$ and $\sigma_a > 0$. It has turned out that the resulting changes arising in the AC threshold voltage U_c are small, in contrast to the DC threshold voltage of EC, which changes by about 25% for the material parameters of the nematic **MBBA**.[51] The wave number $|\boldsymbol{q}_c|$ of the patterns is not much influenced by the inclusion of flexoelectricity in contrast to considerable changes with respect to the direction of the wave vector.
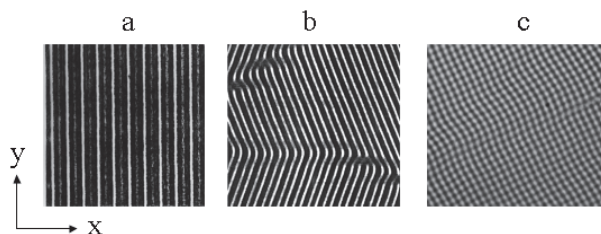
Fig. 4.3. Snapshots of (a) *normal rolls*, (b) *oblique rolls* and (c) *squares*.

In the high frequency (dielectric) regime, however, the flexo-effect becomes much more important, as has been demonstrated more recently. It modifies considerably the threshold and the critical wave vector.[26,30,53] In general, the inclusion of the flexo-effect breaks also the temporal symmetry, in the conductive regime contributions of the dielectric symmetry appear and *vice versa* in the dielectric regime. In Sec. 4.3.1 we will give more details. In addition, it will be discussed why flexoelectricity is really crucial to understand EC for very low frequencies ($\omega\tau_\mathrm{d} \lesssim 1$) and thin cells ($d < 10~\mu$m).

For the parameter combination $\epsilon_a < 0$, $\sigma_a < 0$ that can be found in some nematic compounds, electroconvection is definitely excluded within the standard model. Nevertheless, EC has surprisingly been observed in this case (for recent examples see, e.g. Refs. 17,18). The theoretical analysis has proved, that flexoelectricity is crucial to understand this *nonstandard* EC.[19] The point is that in Eq. (4.7) the contribution $\nabla \cdot \boldsymbol{P}_\mathrm{fl}$ to ρ_{el} becomes dominant. It is interesting that the flexo torque on the director is determined by the difference $(e_1 - e_3)$ of the flexocoefficients while the sum $(e_1 + e_3)$ governs the flexo charge and thus its contribution to the viscous torque. Further details will be sketched in Sec. 4.3.2.

So far we have discussed EC instabilities driven by a sinusoidal AC voltage. When the AC driving voltage $U(t)$ with a period T is "asymmetric", i.e. $U(t + T/2) \neq -U(t)$, one finds besides the conductive and the dielectric a "subharmonic" pattern where the director dynamics is $2T$-periodic in time.[54] The impact of flexo polarization on standard and nonstandard EC in the case of an asymmetric driving voltage has been analyzed as well.[55,56] One recovers in principle the scenarios with symmetric driving described before, except the appearance of subharmonic patterns in the standard EC case.

For completeness we would like to mention that the impact of flexo-electricity has not been analyzed for all material parameter combinations, where EC has been observed in nematics. An overview of the various cases has been given in a recent review,[57] which contains a systematic discussion of the sensitive influence of the sign of the anisotropies ϵ_a, σ_a, and of the basic director configuration on the patterns. For instance in the homeotropic configuration with $\epsilon_a > 0$, $\sigma_a < 0$, isotropic convection (where the roll axis is spontaneously chosen in the EC bifurcation) has been experimentally observed and theoretically analyzed.[58–60] In particular the appearance of square patterns [see Fig. 4.3(c)], which are typical for isotropic convection, is well understood. In general, one finds satisfactory agreement between theory and experiment for this interesting EC scenario without including flexoelectricity.

4.3.1. *Standard electroconvection*

This section deals with the influence of flexoelectricity on electroconvection with planar geometry and the most studied material parameter combination $\epsilon_a < 0$ and $\sigma_a > 0$. The analysis makes use of the common nemato-electrohydrodynamic equations,[2,15] where in addition the flexo polarization is included. This leads to modifications in the electric torques and influences also the charge density ρ_{el} [Eq. (4.7)].[19,48]

In order to have a definite situation, we mainly have used in our analysis the material parameters of **Phase 5**.[30] However, in order to study specifically the impact of the flexoelectricity, a "theoretical" scaling factor ξ has been introduced to tune the strength of flexoelectricity, i.e. we use $\xi_-(e_1 - e_3)$ instead of $(e_1 - e_3)$ and $\xi_+(e_1 + e_3)$ instead of $(e_1 + e_3)$. In Fig. 4.4 the calculated critical voltage $U_c(f)$ as a function of the AC frequency f is shown for three different values of $\xi = \xi_+ = \xi_-$. In line with the standard model, EC with conductive symmetry at low ω switches to "dielectric" EC at a certain crossover frequency ω_c for $\xi = \xi_+ = \xi_- = 0$ (i.e. in the absence of flexoelectricity).

For a finite flexoelectric contribution of realistic magnitude ($\xi = \xi_+ = \xi_- = 1$), the dielectric threshold and the crossover frequency ω_c decrease, while the conductive threshold is not affected significantly. The results of the experiments on **Phase 5** shown in Fig. 4.4 as circles agree very well with the theory. Measuring frequencies in units of the director relaxation time τ_d the range $0 < \omega\tau_d < 140$ is covered in the figure. A closer look reveals a further consequence of the flexoelectricity: the slope of $U_c(f)$ versus
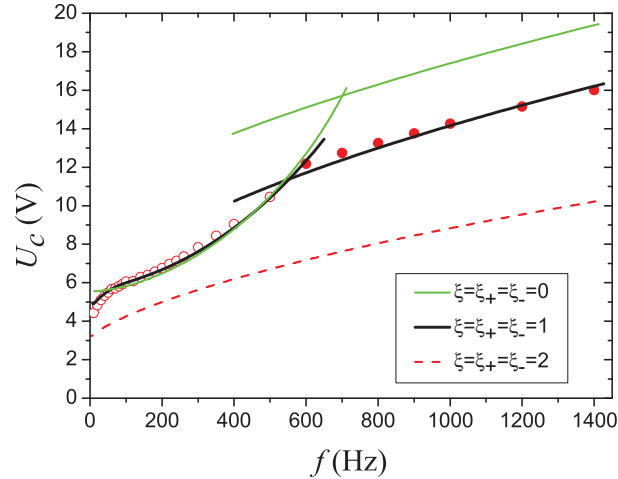
Fig. 4.4. Threshold voltage U_c as a function of the frequency f calculated for **Phase 5** material parameters and for different values of the flexoelectric strength ξ. Circles and bullets represent the experimental data for conductive and dielectric EC, respectively.

f increases quite strongly at small $f < 100$ Hz.[30] If the flexo strength is further increased the dielectric U_c branch expands further towards small frequencies, until the conductive range totally vanishes and EC with dielectric symmetry bifurcates in the whole frequency range. This is documented in Fig. 4.4 for $\xi = \xi_+ = \xi_- = 2$. Similar theoretical curves for U_c as in Fig. 4.4 have been also obtained when choosing **MBBA** material parameters.[26] In contrast to **Phase 5** we find, however, oblique rolls in the dielectric regime (for further details see Ref. 26).

The onset characteristics of planar EC with $\epsilon_a < 0$, $\sigma_a > 0$ depend strongly on the magnitude of σ_a. In the absence of flexoelectricity the crossover frequency ω_c between EC with conductive and dielectric symmetry moves towards $\omega = 0$ when decreasing σ_a. At the same time the critical voltage U_c diverges. For finite e_1, e_3 the shift of ω_c is observed as well but U_c remains finite. This scenario is documented in the upper panel of Fig. 4.5 for **MBBA** material parameters[19] except that a larger flexo strength with $\xi = \xi_+ = \xi_- = 2$ is used and σ_a is varied. Time is measured in units of the charge relaxation time $\tau_q = 4.7 \times 10^{-3}$ s. For $\sigma_a = 0.5$ we have dielectric
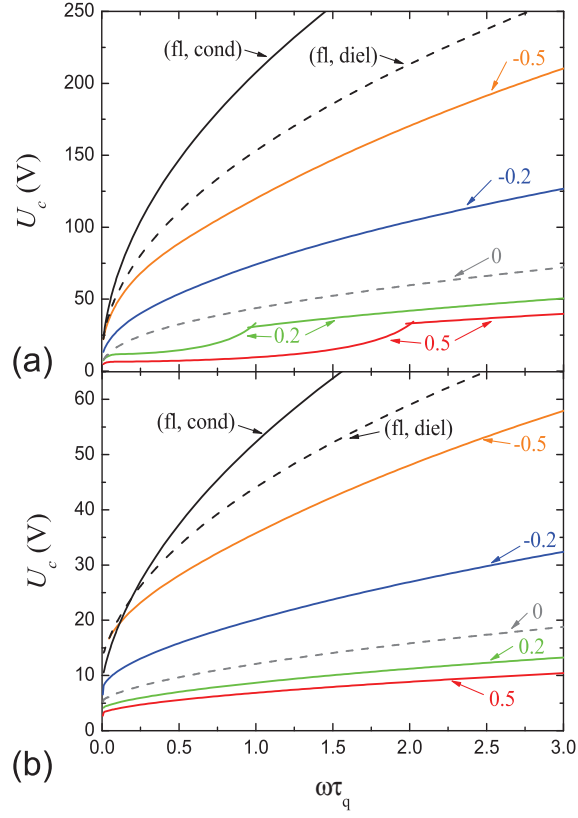
Fig. 4.5. Threshold voltage of EC as a function of the dimensionless frequency $\omega\tau_q$ calculated with **MBBA** material parameters and $\xi = \xi_+ = \xi_- = 2$ for five different values of $\sigma_a/\sigma_\perp$ between 0.5 and -0.5. The corresponding critical voltages for the flexo-domains with conductive symmetry (fl, cond) and with dielectric symmetry (fl, diel) are included as well. (a) Sample thickness $d = 40$ μm; (b) $d = 10$ μm.

rolls for $\omega_c\tau_q > 2$ and conductive rolls for $\omega_c\tau_q < 2$, while $\omega_c\tau_q \approx 1$ for $\sigma_a = 0.2$. For $\sigma_a = 0$ we find dielectric rolls in the whole frequency range. On the other hand U_c has monotonically moved up with decreasing σ_a. The

discussion of the cases $\sigma_a < 0$ is postponed to the following section.

Besides σ_a the cell thickness d of the nematic layer, which has almost no effect in the case $e_1 = e_3 = 0$, reveals a strong influence on EC for finite flexocoefficients. This is demonstrated in the lower panel of Fig. 4.5, where for $d = 10$ μm the conductive branch is totally absent. Then, similarly to the conductive regime, one can find a transition from oblique to normal dielectric rolls above a Lifshitz frequency ω_L. In a recent experiment the oblique dielectric rolls at small ω have indeed been observed.[29] The threshold characteristics U_c, q_c and obliqueness angle α could be well reproduced by a theoretical analysis of the nematohydrodynamic equations including flexo polarization.[29]

Finally we would like to point out, that also the magnitude, σ_0, of the electrical conductivity in nematics plays an important role. In Fig. 4.5 we have chosen $\sigma_0 = 10^{-8}$ $(\Omega$ m$)^{-1}$, which is the typical scale of the electrical conductivities in nematics commonly used in the experiments. A closer look at the linear nemato-electrohydrodynamic equations (see the Appendix of Ref. 19) shows that the thickness d as well as σ_0 appear only through the dimensionless parameter $Q \propto \tau_{\mathrm{d}}/\tau_{\mathrm{q}} \propto \sigma_0 d^2$. Thus decreasing σ_0 by a factor 16 would have been equivalent to the reduction of d by a factor of 4 [compare Fig. 4.5(a) and Fig. 4.5(b)].

In Fig. 4.5 we have also included the (σ_a-independent!) critical voltage curves for flexo-domains of conductive and of dielectric symmetry. They exist for the standard **MBBA** material parameters[26] except that the flexo strength is increased by a factor of two ($\xi = \xi_+ = \xi_- = 2$). Obviously, for finite frequencies the flexo-domains play no role compared to the EC rolls with their much lower U_c values. However, in the limit $\omega \to 0$ both critical voltages decrease and approach each other, which will become important in Sec. 4.4.

4.3.2. *Nonstandard electroconvection*

As already stated before, electroconvection is not explained by the standard model for $\sigma_a < 0$ and $\epsilon_a < 0$. Surprisingly, EC has been observed also for this parameter combination in certain calamitic nematics.[17,18,61–64] These EC patterns differ clearly from the standard EC patterns: the rolls are dominantly parallel to the initial director alignment [see Fig. 4.6(a)]. They are not observable by the common shadowgraph technique (single polarizer) but by using crossed polarizers (plus sometimes an additional $\lambda/4$ plate). The investigation on these "nonstandard EC" rolls has been re-

cently intensified.[18,19,26,30,53,65] Of particular importance are materials for which the conductive anisotropy σ_a changes from negative values to positive ones as function of temperature, whereas the other material parameters do not change much and, in particular, the sign of ϵ_a does not change. Thus simply increasing the temperature gives the excellent opportunity to move continuously from nonstandard EC (ns-EC) to standard EC (s-EC).

In Fig. 4.5 it has been demonstrated that a finite threshold can be obtained for $\sigma_a < 0$ and $\epsilon_a < 0$, when the standard electrohydrodynamic description of nematics is extended by including flexoelectricity; thus nonstandard EC can in fact be explained. According to the theory ns-EC is characterized by the dielectric symmetry and the ns-EC rolls have the orientation almost parallel to the preferred direction $\boldsymbol{n}_0 \parallel \boldsymbol{x}$, in distinct contrast to the s-EC rolls. The critical voltage is predicted to increase almost linearly with ω in contrast to a rise roughly $\propto \sqrt{\omega}$ in standard dielectric electroconvection. These general trends are in satisfactory agreement with the recent experimental findings. Even quantitatively theory and experiments in the standard as well as in the nonstandard regime match very well in some cases.[19] The material parameters are mostly measured in this case and the flexocoefficients e_1, e_3 have been used as fit parameters. It is worth mentioning that in some cases also a Hopf bifurcation to travelling ns-EC rolls has been observed.[18] To describe this scenario flexoelectricity should be incorporated into the weak electrolyte model (WEM),[66] which was able to capture travelling s-EC rolls. This is certainly a demanding task, which would involve a detailed description of the electric conductivity in terms of the participating ions, their mobility and their recombination rates.

Nonstandard EC has been also observed in bent-core nematics,[67–70] where $\sigma_a < 0$, $\epsilon_a < 0$ is also realized and where flexoelectricity is strong. A detailed theoretical description is missing so far. One has to cope with a strong frequency dependence of σ_a,[67] as well as with the unusual viscosity and elastic properties; they might indicate smectic cluster formations not only in the nematic, but even in the isotropic phase.[70–74]

Convective patterns have also been observed long time ago for the $\epsilon_a > 0$ and $\sigma_a > 0$ parameter combination in the case of an initial homeotropic director orientation.[41,75–78] They are observed in a polarizing microscope (crossed polarizers) as an arrangement of "Maltese crosses". The so called isotropic mechanism has been proposed to explain this instability. Alternatively, "Maltese crosses" have been interpreted to be driven by the so called surface polarization mechanism.[79,80] However, the theoretical treatments of both mechanisms are not worked out in detail to allow for comparison
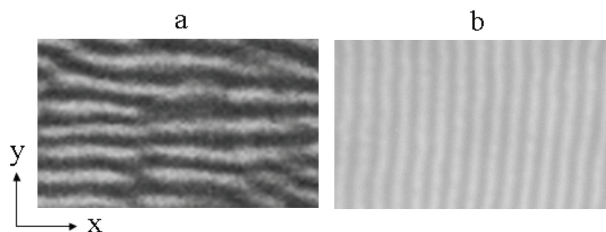
Fig. 4.6. Snapshots of two types of nonstandard EC patterns in planar nematics ($\boldsymbol{n}_0 \parallel \boldsymbol{x}$) with (a) $\epsilon_a < 0$, $\sigma_a < 0$, and (b) with $\epsilon_a > 0$, $\sigma_a > 0$.

with experiments.

It is unclear so far why instead of "Maltese crosses" convective cellular and subsequently roll patterns resulting from a secondary instability have been detected in a recent study.[81] Note that these patterns have been observed both in the homeotropic and in the planar geometry [for the rolls, see Fig. 4.6(b)]. A theoretical analysis is missing so far. In case of a homeotropic alignment the inclusion of flexo polarization into the standard model of EC does not provide mechanisms to drive electroconvection. First, there is no direct flexoelectric torque on the director in this geometry. Second, the flexo charge contribution is too small such that the originating viscous torque cannot overcome the strong stabilizing electric torque, since the substances are characterized by a large $\epsilon_a > 0$. In the planar case the electric torque leads at first to the Freedericksz transition from the planar to the homeotropic orientation of the director, except in a thin boundary layer. So we are essentially back to the homeotropic case where flexoelectricity does not support EC.

4.4. Crossover between flexo-domains and electroconvection

From a basic point of view it is very interesting, that even a crossover between the equilibrium flexo-domains and the dissipative EC patterns can be observed in the same experiment (planar geometry) by just increasing the AC frequency ω. Inspection of Fig. 4.5 already reveals that at very small ω and for suitable material parameter combinations of the nematics, the critical voltage of the equilibrium flexo-domains and that of the dissipative electroconvection patterns might approach each other. In fact, very recent theoretical and experimental studies on the calamitic nematic

Phase 4, have demonstrated the existence of a crossover between these two qualitatively different patterns at a very low transition frequency f_t.[29]

Before discussing these previous experiments we will present new measurements[82] using the nematic **Phase 5** which show a similar crossover at $f_t \lesssim 0.1$ Hz. Thus for $f < f_t$ one has flexo-domains as a first instability while for $f > f_t$ one observes usual EC roll patterns with conductive symmetry. Above the Lifshitz frequency $f_L \approx 40$ Hz one finds normal rolls which are replaced by oblique rolls in the region $f_t < f < f_L$. The cell thickness was $d = 11.3$ μm. Roughly speaking the frequency dependence of U_c is analogous to the lowest curve in Fig. 4.5(a). Detailed studies regarding the main characteristics [such as $U_c(f)$ and $\mathbf{q_c}(f)$] of both patterns are in progress.

Regarding the temporal evolution of the pattern, the contrast $C(t)$ is in general time periodic with a frequency twice the external AC frequency f. It was, however, not expected that the functional form of $C(t)$ would become increasingly spiky when decreasing f [see Fig. 4.7(d)]. In a recent theoretical study it has been shown that such a behaviour is generic for flexo-domains and also for EC rolls at frequencies $\omega\tau_\mathrm{d} < 1$.[26] Both patterns are indeed expressed in Fig. 4.7(d), where $C(t)$ is shown over one period $T = 1/f = 10$ s. In the interval $T/2 < t < T$ the first maximum (a) of $C(t)$ corresponds to the longitudinal flexo-domains [Fig. 4.7(a)], then the contrast decays and remains on a flat plateau (b) value [Fig. 4.7(b)], i.e. the nematic is in the quiescent state. Afterwards oblique EC rolls appear which is reflected in a second steep maximum (c) of $C(t)$ [Fig. 4.7(c)]. The whole sequence repeats itself periodically. At the moment it is unclear, why in particular the flexo-domain peak in the interval $0 < t < T/2$ is much less expressed than in the interval $T/2 < t < T$. Asymmetries in the boundary conditions (e.g. pre-tilt) come immediately into mind. Moreover, even a small DC offset in the applied AC voltage, which practically would not change the threshold values of U_c and $\boldsymbol{q}_c$, could lead to a strong asymmetry of the $C(t)$ peaks over one AC period in the spiky regime.

The transition between the flexo-domains and the conductive oblique EC rolls within the period T has also been confirmed in Fourier space by light diffraction experiments.[82] The incoming light beam had nearly normal incidence and the fringes have been recorded on a screen at a distance of about 0.6 m from the sample. Flexo-domains [Fig. 4.7(a)], which are oriented along $\boldsymbol{n}_0 \parallel \boldsymbol{x}$, produce obviously a set of fringes along the y-axis as shown in Fig. 4.8, left panel. The zig and zag oblique roll patches visible in Fig. 4.7(c) are directly responsible for the set of fringes along the two
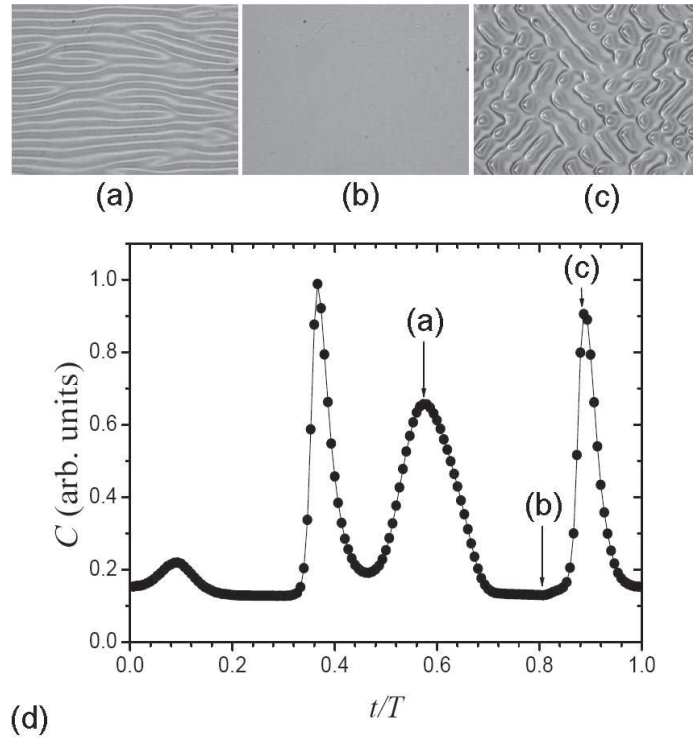
Fig. 4.7.   Flexo-domains (a), quiescent state (b), and conductive oblique EC rolls (c) in **Phase 5**. The initial director is horizontal. (d) Temporal evolution of the contrast C within a period T of the driving voltage above the onset of instabilities at $f = 0.1$ Hz, close to the transition frequency f_t. Arrows indicate the time instant when the snapshots in the corresponding subfigures were taken.

lines through the origin that include an angle 2α; here α denotes the angle between the wave vector of the rolls and the $x-$axis (Fig. 4.8, right panel). The fringes along the $x, y-$axes in Fourier space (Fig. 4.8, right panel) are due to nonlinear effects; they correspond to the sum and difference of the zig and zag wave vectors.[50] A detailed theoretical analysis of the competition between flexo-domains and the conductive EC rolls is missing so far.

The competition of *dielectric* oblique EC rolls and flexo-domains has recently been studied by using the nematic **Phase 4**,[29] which had a low electric conductivity σ_0. The cell thickness was $d = 11.4$ μm. Obviously the constellation of the various material parameters is such, that the sce-
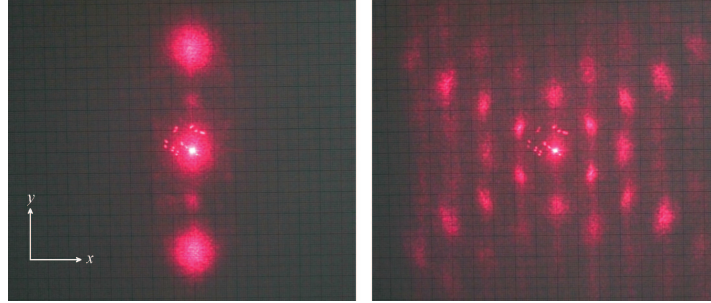
Fig. 4.8.   Light diffraction patterns for flexo-domains (left) and for conductive oblique EC rolls (right) at different instants within the same period of the driving voltage, slightly above the onset of the instabilities and at $f = 0.1$ Hz (close to the transition frequency f_t).

nario in Fig. 4.5(b) is realized, where only dielectric EC rolls exist near onset for positive values of $\sigma_a/\sigma_\perp$. For frequencies above the Lifshitz frequency, $f_L = 50$ Hz, one finds normal dielectric rolls and for $f < f_L$ oblique ones. The transition to flexo-domains is observed at $f_t \approx 0.1$ Hz. It has been demonstrated in a recent theoretical analysis[26] that such a scenario is possible within the nemato-electrohydrodynamic equations including flexo polarization.

In Fig. 4.9 we present the critical voltage U_c, the critical wave length λ and the angle of obliqueness α of the rolls at onset. The latter quantity reflects in particular the transition from the longitudinal flexo-domains ($f < f_t$) with $\alpha = 90°$ to the oblique EC rolls ($f > f_t$) with much smaller α.

Since not all material parameters are known for **Phase 4**, certain fitting procedures have been used in the theoretical analysis. In particular the flexocoefficients have been chosen in such a way, that the theoretical curves for the critical data (U_c, $\boldsymbol{q}_c$) at larger f, i.e. for 5 Hz $< f <$ 200 Hz have agreed very well with the experimental ones (not shown here). It has then been very satisfactory to see an internal consistency: the experimental and the theoretical DC critical voltage for flexo-domains calculated with the same parameters agreed very well.

It should be stressed that the curving up of U_c for the EC rolls in Fig. 4.9(a) when approaching f_t, cannot be described by the existing theories. It seems to be very plausible, that at very small f the measured U_c has to be corrected by contributions due to alignment coatings on the confining electrode plates and from Debye screening layers at the boundaries. Some
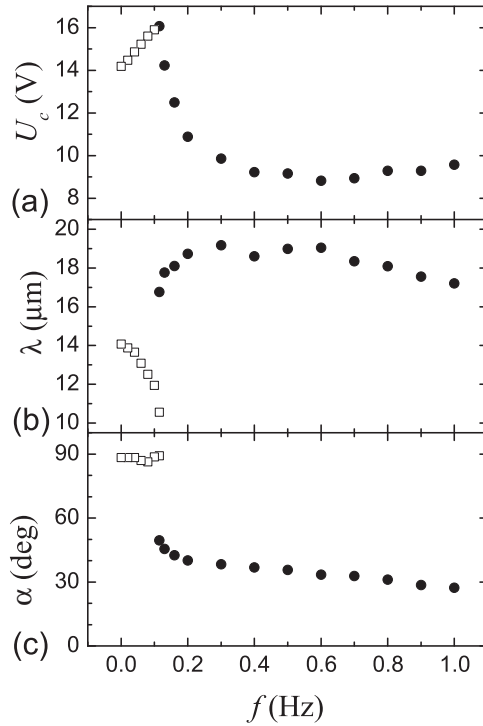
Fig. 4.9. The threshold voltage U_c (a), the wavelength λ (b), and the angle of obliqueness α (c) as a function of driving frequency f for flexo-domains ($\square$) and for oblique dielectric EC rolls ($\bullet$) in **Phase 4**.

additional remarks are postponed to the following section 4.5.

4.5. Discussions and conclusions

Convection instabilities in simple isotropic fluids, like Rayleigh-Bénard convection (for a recent review see Ref. 83), are completely understood near onset, also because the number of relevant material parameters is fairly small. In contrast, pattern-forming instabilities in nematic liquid crystals are very rich as also documented in this review; their detailed exploration, however, requires the demanding numerical analysis of the complex nemato-

electrohydrodynamic equations and therefore the knowledge of much more material parameters. Some of them, like the dielectric permittivities or the electric conductivities are relatively easy to measure, which does not apply, however, to all the five viscosity coefficients α_i in nematics.[2] Most difficult is the determination of the flexocoefficients, which play a central role in this chapter. In general, the flexocoefficients have been obtained only for few substances by purposefully directed measurements. Therefore we will discuss here, how the analysis of the pattern-forming instabilities described in this chapter can contribute to the determination of flexocoefficients.

We note first that according to Eqs. (4.1) and (4.2), simultaneously reversing the signs of e_1, e_3, and $\boldsymbol{E}$ does not change the flexoelectric torque on the director. The same holds for the total torque too, as the elastic and viscous contributions are independent of $\boldsymbol{E}$, while the dielectric one depends only on $\boldsymbol{E}^2$. Consequently, the resulting patterns are also invariant with respect to the same transformation. On the other hand, inspection of the general electrohydrodynamic equations shows that at least the threshold characteristics of the flexo-domains (and also of the electroconvection patterns) are independent of the sign of $\boldsymbol{E}$ and hence these characteristics would also remain unaltered if the signs of both flexocoefficients are inverted together. Consequently only the relative signs of e_1 and e_3 can be extracted from analysing the flexoelectric or EC patterns.

Let us now first concentrate on the flexo-domains. With the help of the general theory[26] $|e_1 - e_3|$ can be determined from the measurements of U_c and q_c of the flexo-domains if the elastic coefficients K_1, K_2, and the anisotropy ϵ_a are known. In this way the value of $|e_1 - e_3| = 5.7$ pC/m has been obtained[11,12] for **BMAOB**. Note that this value has been confirmed in the case of a twisted cell geometry.[38] In a later study **BMAOB** doped with a "swallow-tail" compound in concentrations up to 4.55 mole% has been analyzed.[84] The value of $|e_1 - e_3|$ for the mixture has been found to be slightly increased with increasing concentration of the "swallow-tail" compound (see Fig. 6 in Ref. 84).

It is interesting that flexo-domains have also been detected in a *metallo-organic* nematic liquid crystal which has been obtained by complexation with palladium.[85] The value of $|e_1 - e_3|$ has been found of the same order of magnitude as in usual nematics.[25,78]

As already indicated in Chapter 2 of this book,[44] different measurements may show large discrepancies in the values of flexocoefficients. This becomes evident when one considers for instance **MBBA**, one of the mostly used nematics in our context. According to the "standard" data set[19,51]

where $e_1 - e_3 = 4$ pC/m, $\delta k = 0.23$, one does not expect flexo-domains since $\mu = -1.6 < \mu_{min}(\delta k) = -0.8$ in Fig. 4.2. In fact flexo-domains have not been reported in most experiments. In few cases, however, flexo-domains have been observed for **MBBA** both in the standard planar geometry[47,86] as well as in the hybrid (planar-homeotropic, HAN) configuration,[39] where they should be excluded as well. Would one increase, however, the difference $|e_1 - e_3|$ by a factor of about two, flexo-domains are immediately allowed ($\mu = -0.4 > \mu_{min}$ in Fig. 4.2). A look at the report comparing the various measurements of the e_1, e_3 in **MBBA**,[87] as well as at Table A.1 in Appendix A, shows that the smallest values of $|e_1 - e_3|$ and the largest ones differ even by a factor of about 4.5 there.

For completeness we would like to mention some studies on flexo-domains in **BMAOB** under the *combined action of DC and high frequency AC voltages*.[33,88] It has been found that the critical DC voltage and the critical wave number of the patterns are increased when increasing the AC voltage. On the basis of the standard director equations these findings are very plausible. The quantitative analysis in Refs. 33 and 88, however, suffers from the same mistake as reported recently for the pure DC case.[34] Thus the estimation of the flexocoefficients in these papers is not convincing.

Another complication is the finite, though very small electric conductivity of most nematics, which easily leads to material flow. This has been systematically measured for flexo-domains in the HAN geometry[39] above onset by following the trajectories of tracer particles. In general we expect, that the existence of flow will lead to perturbations of the ideal flexo-domain patterns for instance by the generation of defects, like dislocations and disclinations.

As we already mentioned, measurements of the critical voltage U_c and the critical wave number q_c of flexo-domains in the DC case allow to obtain an estimate of the magnitude of $e_1 - e_3$, but not its sign. In principle much more information is contained in the EC pattern, since the frequency serves as an important secondary control parameter besides the voltage amplitude, and the sum $e_1 + e_3$ can also be tested. As documented in Sec. 4.3.1 for s-EC, the location of the Lifshitz frequency or the sensitive dependence of the U_c, $\boldsymbol{q}_c$ curves on ω in the dielectric regime give valuable insights. Moreover, materials, where a transition between flexo-domains and EC exists, are of particular interest, since both the difference and the sum of e_1 and e_3 can be extracted.

For instance from fits (based on the extended standard model of EC in-

cluding flexoelectricity) to the experimental EC threshold voltages $U_c(\omega)$, for **Phase 4** one finds $e_1 - e_3 = -4.7$ pC/m and $e_1 + e_3 = -31.5$ pC/m.[29] The difference $e_1 - e_3$ corresponds to $\mu = -0.3$ ($\delta k = 0.21$) which is inside the existence regime of the flexo-domains (see Fig. 4.2) and indeed flexo-domains were seen. From independently measuring their U_c and q_c values, $|e_1 - e_3| = 4.7$ pC/m and $|e_1 - e_3| = 4.1$ pC/m have been obtained, respectively; they match nicely with the EC fit value. From similar EC fits one finds for **Phase 5** the values $e_1 - e_3 = -2.9$ pC/m, $e_1 + e_3 = -50.1$ pC/m, and for **MBBA** $e_1 - e_3 = 6.0$ pC/m, $e_1 + e_3 = -35.0$ pC/m.[30] In this latter case the difference $e_1 - e_3$ for **MBBA** corresponds to $\mu = -0.6$ which is slightly larger than $\mu_{min} = -0.8$; thus we would be inside the existence regime of the flexo-domains (see Fig. 4.2). Note, that U_c and $\boldsymbol{q}_c$ of the EC pattern are insensitive against the sign inversion of both flexocoefficients, as already mentioned earlier in this section. Thus the EC fits can provide only the relative signs of $e_1 - e_3$ and $e_1 + e_3$.

Finally, we mention that the longitudinal rolls observed in a *bent-core* nematic have been associated in Ref. 67 with ns-EC patterns. In a recent paper,[89] however, similar patterns have been interpreted as flexo-domains and in this way the value of $|e_1 - e_3| \approx 6$ pC/m has been estimated. This value is of the same order of magnitude as in calamitic nematics. Similarly, for the flexocoefficients of another bent-core nematic a value of $O(10\,\mathrm{pC/m})$ has been obtained by studying the instability due to the surface polarization mechanism.[90]

In any case, EC measurements should be used as a test bed and a consistency check for the various methods described in Chapter 2 of this book[44] where the flexocoefficients are directly measured by appropriate deformations of a homogeneous nematic layer.

While the linear description of flexo-domains which yields q_c and U_c is quite well worked out in theory, the weakly nonlinear regime and the secondary bifurcations from the flexo-domains have not yet been explored. This is certainly a rewarding problem in view of the interesting patterns observed for instance in experiments in a DC electric field. In addition, the secondary bifurcations are much more sensitive to the values of the material parameters as the first instability. If the nematic is practically an insulator, the flexo-domains are reported to be stable for applied DC voltages U considerably larger than U_c.[8] For higher electric conductivities, however, flexo-domains have been found to be destabilized by EC rolls in **MBBA** when increasing DC voltage.[39,45,86] As it should be, the EC rolls are oriented perpendicular to the preferred director orientation, i.e.

perpendicular to the orientations of the flexo-domains (see, e.g. Fig. 9 in Ref. 45). Without detailed calculations this scenario allows for a simple qualitative explanation. The optimal action of the Carr-Helfrich mechanism is prohibited by the distortions of the underlying director structure in the flexo-domains where n_z and n_y vary periodically along the $y-$direction. The n_y modulations are considered to be less prohibitive for EC, as also evident from the existence of the so called *abnormal* EC rolls.[49,91] They are characterized by the common, spatially periodic n_z distortions in the presence of a spatially homogeneous n_y distortion. Thus it is not surprising, that the transverse EC rolls are restricted to the regions where $|n_y| > |n_z|$ and thus would not run continuously through the flexo-domains. Note, that the same scenario has also been observed in the secondary bifurcations of the flexo-domains in the HAN geometry.[39]

The analysis in the case of an alternating appearance of flexo-domains and EC patterns at low AC frequencies discussed in Sec. 4.4 is much more complicated. For frequencies $f \approx f_t$, where the threshold voltages of both patterns are near to each other, one expects them to flash up independently at onset. With increasing voltage flexo-domains and rolls will start to interact, apart from the fact that each pattern type might develop its own secondary instabilities. To disentangle these processes is certainly a very demanding task, both in theory and in experiments.

In the theoretical analysis of electrically driven pattern formation in nematics one deals only with the "theoretical" AC voltage U_{theo} which drops over the nematic layer. U_{theo} differs, however, from the "experimental" voltage U_{exp} applied to the whole LC-cell and recorded in the experiments. Thus a quantitative comparison between the experiments and the theory is far from trivial, as it has been emphasized for instance in Ref. 26. Typical liquid crystal cells consist of a nematic layer confined between ITO- or SnO_2-coated glass plates covered with a thin film of an aligning polymer. As the polymer is a quite good insulator, this sandwich possesses fairly complicated electric properties. In particular, at low frequencies the whole system has to be represented by a complex equivalent electric circuit model.[92,93]

Furthermore, the ionic character of the electric conductivity of nematics, which in many cases is satisfactorily described through a simple ohmic conductivity, becomes certainly important at low ω. Debye screening layers build up in the nematic near the electrodes, where part of the applied voltage drops as well. This happens only if the ions are able to follow the external driving. It is easy to see that a new characteristic time $\tau_{\mathrm{mig}} \propto d^2$,

which is needed to form the Debye layer, comes into play.[66] The Debye layer and the voltage drop across it are considered to be important only for frequencies $\omega\tau_{\mathrm{mig}} < 1$. This additional voltage drop is most probably relevant in explaining the curving up of the measured U_{exp} at low frequencies and small d.[29,30] Given that U_{theo} mostly decays monotonically with decreasing ω (for an exception see the next paragraph below), a minimum of U_{exp} at $\omega_{min} \sim \tau_{\mathrm{mig}}^{-1} \propto d^{-2}$ is expected. In fact a minimum and a subsequent curving up of $U_{exp}(\omega)$ has been observed in the experiments.[29,30] For thin cells the proportionality $\omega_{min} \propto d^{-2}$ has been confirmed as well. The question remains whether this thickness dependence originates really from τ_{mig}^{-1} or from the inverse director relaxation time ($\tau_{\mathrm{d}}^{-1} \propto d^{-2}$) as proposed in Ref. 30. There the relation $\omega_{min} \approx 2\pi\tau_{\mathrm{d}}^{-1}$ has been found for $2~\mu\mathrm{m} \leq d \leq 10~\mu\mathrm{m}$ in **Phase 5**. In Ref. 29, however, a much smaller proportionality factor has been measured in **Phase 4** since $\omega_{min} \approx 0.2\tau_{\mathrm{d}}^{-1}$ for $d = 11.4~\mu\mathrm{m}$.

Note that in Ref. 30 the curving up of U_{exp} has tentatively been associated with increase of U_{theo} at low ω. Such a dependence of U_{theo} has been found in simulations only for small ratios $\sigma_a/\sigma_\perp \lesssim 0.1$, however, the nematic used in Ref. 30 had $\sigma_a/\sigma_\perp = 0.7$.

In summary, we have shown that the flexo polarization has a strong impact on the pattern-forming instabilities in nematics subjected to the action of an electric field. This applies not only to flexo-domains but also to EC patterns. In the present stage the theoretical analysis of the nemato-electrohydrodynamic equations in the linear regime allows to calculate the critical voltage and the critical wave vector of the patterns. For better quantitative comparison with the experiments one would need a more precise knowledge of the various material parameters, in particular, of the crucial flexocoefficients e_1 and e_3. For that purpose more experiments with stable nematics, that show both flexo-domains and EC patterns, are most welcome. In particular systematic studies with respect to the frequency, the thickness, and electric conductivity dependencies of the patterns are of great importance. Certainly finding chemically stable nematics with small dielectric anisotropy and low electric conductivity would allow a big step forward.

Acknowledgements

References

1. A. Buka, and L. Kramer, Eds., *Pattern Formation in Liquid Crystals.* (Springer-Verlag, New York, 1996).

2. P. G de Gennes, and J. Prost, *The Physics of Liquid Crystals.* (Clarendon Press, Oxford, 1993).

3. F. Lonberg, and R. B. Meyer, New ground state for the splay-Freedericksz transition in a polymer nematic liquid crystal, *Phys. Rev. Lett.* **55**(7), 718–721, (1985). doi: 10.1103/PhysRevLett.55.718

4. R. B. Meyer, Piezoelectric effects in liquid crystals, *Phys. Rev. Lett.* **22**(18), 918–921, (1969). doi: 10.1103/PhysRevLett.22.918

5. J. Prost, and J. P. Marcerou, On the microscopic interpretation of flexoelectricity, *J. Phys. (France)* **38**(3), 315–324 (1977).
doi: 10.1051/jphys:01977003803031500

6. M. A. Osipov, Chapter 1. Molecular Theory of Flexoelectricity in Nematic Liquid Crystals. In eds. Á. Buka, and N. Éber, *Flexoelectricity in Liquid Crystals. Theory, Experiments and Applications.* (Imperial College Press, London, 2012). pp. 9–32.

7. C. V. Brown, and N. J. Mottram, Influence of flexoelectricity above the nematic Freedericksz transition, *Phys. Rev. E* **68**(3), 031702/1–5, (2003). doi: 10.1103/PhysRevE.68.031702

8. L. K. Vistin', Electrostructural effect and optical properties of a certain class of liquid crystals and their binary mixtures, *Sov. Phys. Crystallogr.* **15**(3), 514–515, (1970) [*Kristallografiya* **15**(3), 594–595, (1970)].

9. L. K. Vistin', New electrostructural effect in liquid crystals of nematic type, *Sov. Phys. Dokl.* **15**(10), 908–910, (1971) [*Dokl. Akad. Nauk SSSR* **194**(6), 1318–1321, (1970)].

10. Yu. P. Bobylev, and S. A. Pikin, Threshold piezoelectric instability in a liquid crystal, *Sov. Phys. JETP* **45**(1), 195–198, (1977) [*Zh. Eksp. Teor. Fiz.* **72**(1), 369–374, (1977)].

11. M. I. Barnik, L. M. Blinov, A. N. Trufanov, and B. A. Umanski, Flexoelectric domains in nematic liquid crystals, *Sov. Phys. JETP* **46**(5), 1016–1019, (1977) [*Zh. Eksp. Teor. Fiz.* **73**(5), 1936–1943, (1977)].

12. M. I. Barnik, L. M. Blinov, A. N. Trufanov, and B. A. Umanski, Flexoelectric domains in liquid crystals, *J. Phys. (France)* **39**(4), 417–422, (1978). doi: 10.1051/jphys:01978003904041700

13. E. F. Carr, Influence of electric fields on the molecular alignment in the liquid crystal p-(anisalamino)-phenyl acetate, *Mol. Cryst. Liq. Cryst.* **7**(1), 253–268, (1969). doi: 10.1080/15421406908084876

14. W. Helfrich, Conduction-induced alignment of nematic liquid crystals: basic model and stability considerations, *J. Chem. Phys.* **51**(9), 4092–4105, (1969). doi: 10.1063/1.1672632

15. E. Bodenschatz, W. Zimmermann, and L. Kramer, On electrically driven pattern-forming instabilities in planar nematics, *J. Phys. (France)* **49**(11), 1875–1899, (1988). doi: 10.1051/jphys:0198800490110187500

16. L. Kramer, and W. Pesch, *Electrohydrodynamic instabilities in nematic liq-*

uid crystals. In eds. Á. Buka, and L. Kramer, *Pattern Formation in Liquid Crystals.* pp. 221-256. (Springer-Verlag, New York, 1996).

17. E. Kochowska, S. Németh, G. Pelzl, and Á. Buka, Electroconvection with and without the Carr-Helfrich effect in a series of nematic liquid crystals, *Phys. Rev. E* **70**(1), 011711/1–9, (2004). doi: 10.1103/PhysRevE.70.011711

18. T. Tóth-Katona, A. Cauquil-Vergnes, N. Éber, and Á. Buka, Nonstandard electroconvection with Hopf bifurcation in a nematic liquid crystal with negative electric anisotropies, *Phys. Rev. E* **75**(6), 066210/1–12, (2007). doi: 10.1103/PhysRevE.75.066210

19. A. Krekhov, W. Pesch, N. Éber, T. Tóth-Katona, and Á. Buka, Nonstandard electroconvection and flexoelectricity in nematic liquid crystals, *Phys. Rᵉᵛ E* **77**(2), 021705/1–11, (2008). doi: 10.1103/PhysRevE.77.021705

20. Á. Buka, and L. Kramer, Theory of nonlinear transient patterns in the sp Freedericksz transition, *Phys. Rev. A* **45**(8), 5624–5631, (1992). doi: 10.1103/PhysRevA.45.5624

21. Á. Buka, and L. Kramer, Linear and non-linear transient patterns in the splay Freedericksz transition of nematics, *J. Phys. II (France)* **2**(3), 315–326, (1992). doi: 10.1051/jp2:1992136

22. N. Éber, S. A. Rozanski, S. Németh, Á. Buka, W. Pesch, and L. Kramer, Decay of spatially periodic patterns in a nematic liquid crystal, *Phys. Rev. E.* **70**(6), 061706/1–8, (2004). doi: 10.1103/PhysRevE.70.061706

23. W. Pesch, L. Kramer, N. Éber, and Á. Buka, The role of initial conditions in the decay of spatially periodic patterns in a nematic liquid crystal, *Phys. Rev. E.* **73**(6), 061705/1–10, (2006). doi: 10.1103/PhysRevE.73.061705

24. Y. P. Bobylev, V. G. Chigrinov, and S. A. Pikin, Threshold flexoelectric effect in nematic liquid crystal, *J. Phys. Coll. (France)* **40**(C3), C3 331–333, (1979). doi: 10.1051/jphyscol:1979364

25. S. A. Pikin, *Structural Transformations in Liquid Crystals.* (Gordon and Breach Science Publishers, 1991).

26. A. Krekhov, W. Pesch, and Á. Buka, Flexoelectricity and pattern formation in nematic liquid crystals, *Phys. Rev. E* **83**(5), 051706/1–13, (2011). doi: 10.1103/PhysRevE.83.051706

27. C. Oldano, Comment on "New ground state for the splay-Fredericksz transition in a polymer nematic liquid crystal", *Phys. Rev. Lett.* **56**(10), 1098–1098 (1986). doi: 10.1103/PhysRevLett.56.1098

28. W. Zimmermann, and L. Kramer, Periodic splay-twist Fredericksz transition in nematic liquid crystals, *Phys. Rev. Lett.* **56**(24), 2655–2655, (1986). doi: 10.1103/PhysRevLett.56.2655

29. M. May, W. Schöpf, I. Rehberg, A. Krekhov, and Á. Buka, Transition from longitudinal to transversal patterns in an anisotropic system, *Phys. Rev. E* **78**(4), 046215/1–9, (2008). doi: 10.1103/PhysRevE.78.046215

30. T. Tóth-Katona, N. Éber, Á. Buka, and A. Krekhov, Flexoelectricity and competition of time scales in electroconvection, *Phys. Rev. E* **78**(3), 036306/1–12, (2008). doi: 10.1103/PhysRevE.78.036306

31. G. Derfel, and M. Buczkowska, Numerical study of flexoelectric longitudinal

domains, Mol. Cryst. Liq. Cryst. **547**(1), 213–221, (2011).
doi: 10.1080/15421406.2011.572787

32. Y. G. Marinov, and H. P. Hinov, On the threshold characteristics of the flexoelectric domains arising in a homogeneous electric field: the case of anisotropic elasticity, *Eur. Phys. J. E* **31**(2), 179–189, (2010).
doi: 10.1140/epje/i2010-10560-0

33. H. P. Hinov, and Y. Marinov, Theoretical considerations and experimental illustration of the electro-optic behavior of longitudinal flexoelectric domains under the joint action of DC and AC voltages: the case of strong anchoring, *Mol. Cryst. Liq. Cryst.* **503**(1), 45–68, (2009).
doi: 10.1080/15421400902841494

34. A. Krekhov, W. Pesch, and Á. Buka, Comment on "On the threshold characteristics of the flexoelectric domains arising in a homogeneous electric field: the case of anisotropic elasticity" by Y. G. Marinov and H. P. Hinov, *Eur. Phys. J. E* **34**(8), 80/1–2, (2011). doi: 10.1140/epje/i2011-11080-1

35. P. Schiller, G. Pelzl, and D. Demus, Analytical theory for flexo-electric domains in nematic layer, *Cryst. Res. Technol.* **25**(1), 111–116, (1990).
doi: 10.1002/crat.2170250121

36. M. F. Lednei, and I. P. Pinkevich, Threshold spatially periodic structure of the director in a nematic flexoelectric cell with finite anchoring energy, *Crystallography Rep.* **50**(3), 471–477, (2005) [*Kristallografiya* **50**, 517–523, (2005)]. doi: 10.1134/1.1927612

37. M. Ledney, and I. Pinkevych, Influence of anchoring at a nematic cell surface on threshold spatially periodic reorientation of a director, *Liq. Cryst.* **34**(5), 577–583, (2007). doi: 10.1080/02678290500248160

38. B. A. Umanskii, V. G. Chigrinov, L. M. Blinov, and Y. B. Podyachev, Flexoelectric effect in twisted liquid-crystal structures, *Sov. Phys. JETP* **54**(4), 694–699, (1981) [*Zh. Eksp. Teor. Fiz.* **81**(4), 1307–1317, (1981)].

39. V. A. Delev, A. P. Krekhov, and L. Kramer, Crossover between flexoelectric stripe patterns and electroconvection in hybrid aligned nematics, *Mol. Cryst. Liq. Cryst.* **366**(1), 849–856 (2001). doi: 10.1080/10587250108024026

40. S. P. Palto, N. J. Mottram, and M. A. Osipov, Flexoelectric instability and spontaneous chiral-symmetry breaking in a nematic liquid crystal with asymmetric boundary conditions, *Phys. Rev. E* **75**(6), 061707/1–8, (2007).
doi: 10.1103/PhysRevE.75.061707

41. M. I. Barnik, L. M. Blinov, S. A. Pikin, and A. N. Trufanov, Instability mechanism in the nematic and isotropic phases of liquid crystals with positive dielectric anisotropy, *Sov. Phys. JETP* **45**(2), 396-398, (1977). [*Zh. Eksp. Teor. Fiz.* **72**(2), 756–761, (1977)].

42. Kh. Khinov, L. K. Vistin', and Yu. G. Magakova, The flexoelectric character of longitudinal domains in liquid crystals, *Sov. Phys. Crystallogr.* **23**(3), 323–325, (1978) [*Kristallografiya* **23**(3), 583–587, (1978)].

43. P. Kumar, and K. S. Krishnamurthy, Gradient flexoelectric switching response in a nematic phenyl benzoate, *Liq. Cryst.* **34**(2), 257–266, (2007).
doi: 10.1080/02678290601111192

44. N. V. Madhusudana, Chapter 2. Flexoelectro-optics and Measurements of

Flexocoefficients. In eds. Á. Buka, and N. Éber, *Flexoelectricity in Liquid Crystals. Theory, Experiments and Applications.* (Imperial College Press, London, 2012). pp. 33–60.

45. H. P. Hinov, and L. K. Vistin, Parallel and cross-like domains due to d.c. and low frequency (< 2 Hz) electric fields in nematic liquid crystal layers with negative dielectric anisotropy, *J. Phys. (France)* **40**(3), 269–292, (1979). doi: 10.1051/jphys:01979004003026900

46. H. P. Hinov, I. Bivas, M. D. Mitov, K. Shoumarov, and Y. Marinov, A further experimental study of parallel surface-induced flexoelectric domains (PSIFED) (flexo-dielectric walls), *Liq. Cryst.* **30**(11), 1293–1317, (2003). doi: 10.1080/02678290310001607198

47. H. P. Hinov, On the coexistence of the flexo-dielectric walls–flexoelectric domains for the nematic MBBA – A new estimation of the modulus of the difference between the flexoelectric coefficients of splay and bend $|e_{1z} - e_{3x}|$, *Mol. Cryst. Liq. Cryst.* **524**(1), 26–35, (2010). doi: 10.1080/15421400903568161

48. L. Kramer, and W. Pesch, *Electrohydrodynamics in nematics.* In eds. D. A. Dummur, A. Fukuda, and G. R. Luckhurst, *Physical Properties of Nematic Liquid Crystals.* pp. 441–454. (Inspec, London, 2001).

49. À. Buka, N. Éber, W. Pesch, and L. Kramer, Isotropic and anisotropic electroconvection, *Phys. Rep.* **448**(5-6), 115–132, (2007). doi: 10.1016/j.physrep.2007.02.013

50. M. Dennin, D. S. Cannell, and G. Ahlers, Patterns of electroconvection in a nematic liquid crystal, *Phys. Rev. E* **57**(1), 638–649, (1998). doi: 10.1103/PhysRevE.57.638

51. W. Thom, W. Zimmermann, and L. Kramer, The influence of the flexoelectric effect on the electrohydrodynamic instability in nematics, *Liq. Cryst.* **4**(3), 309–316, (1989). doi: 10.1080/02678298908029184

52. N. V. Madhusudana, and V. A. Raghunathan, Influence of flexoelectricity on electrohydrodynamic instabilities in nematics, *Liq. Cryst.* **5**(6), 1789–1812, (1989) doi: 10.1080/02678298908045689; *Mol. Cryst. Liq. Cryst. Lett.* **5**(6), 201–209, (1988).

53. T. Tóth-Katona, N. Éber, and Á. Buka, Flexoelectricity in electroconvection, *Mol. Cryst. Liq. Cryst.* **511**(1), 11–24, (2009). doi: 10.1080/15421400903048461

54. T. John, J. Heuer, and R. Stannarius, Influence of excitation wave forms and frequencies on the fundamental time symmetry of the system dynamics studied in nematic electroconvection, *Phys. Rev. E* **71**(5), 056307-10, (2005). doi: 10.1103/PhysRevE.71.056307

55. J. Low, and S. J. Hogan, Subharmonic pattern formation in a nematic cell – a 1d flexoelectric model approach, *Mol. Cryst. Liq. Cryst.* **478**(1), 67–81, (2007). doi: 10.1080/15421400701735640

56. J. Low, and S. J. Hogan, Standard and nonstandard nematic electrohydrodynamic convection in the presence of asymmetric ac electric fields, *Phys. Rev. E* **78**(4), 041706-15, (2008). doi: 10.1103/PhysRevE.78.041706

57. Á. Buka, N. Éber, W. Pesch, and L. Kramer, *Convective patterns in liquid*

crystals driven by electric field. In eds. A. A. Golovin, and A. A. Nepom-nyashchy, *Self Assembly, Pattern Formation and Growth Phenomena in Nano-Systems.* pp. 55–82. (Springer, Dordrecht, 2006).

58. Á. Buka, B. Dressel, W. Otowski, K. Camara, T. Tóth-Katona, L. Kramer, J. Lindau, G. Pelzl, and W. Pesch, Electroconvection in nematic liquid crystals with positive dielectric and negative conductivity anisotropy, *Phys. Rev. E* **66**(5), 051713/1–8, (2002). doi: 10.1103/PhysRevE.66.051713

59. Á. Buka, B. Dressel, L. Kramer, and W. Pesch, Isotropic convection scenarios in an anisotropic fluid, *Phys. Rev. Lett.* **93**(4), 044502/1–4, (2004). doi: 10.1103/PhysRevLett.93.044502

60. Á. Buka, B. Dressel, L. Kramer, and W. Pesch, Direct transition to electro-convection in a homeotropic nematic liquid crystal, *Chaos* **14**(3), 793–802, (2004). doi: 10.1063/1.1774412

61. M. Goscianski, and L. Leger, Electrohydrodynamic instabilities above a ne-matic to smectic A (or C) transition, *J. Phys. Coll. (France)* **36**(C1), C1 231–236, (1975). doi: 10.1051/jphyscol:1975141

62. N. A. Tikhomirova, A. V. Ginzberg, E. A. Kirsanov, Yu. P. Bobyshev, S. A. Pikin, and P. V. Adomenas, Concerning a new type of instability in liquid crystals, *JETP Lett.* **24**(5), 269–272 (1976) [*Pis'ma Zh. Eksp. Teor. Fiz.* **24**(5), 301–304, (1976)].

63. L. M. Blinov, M. I. Barnik, V. T. Lazareva, and A. N. Trufanov, Electrohy-drodynamic instabilities in the liquid crystalline phases with smectic order-ing, *J. Phys. Coll. (France)* **40**(C3), C3 263–268, (1979). doi: 10.1051/jphyscol:1979350

64. H. R. Brand, C. Fradin, P. L. Finn, W. Pesch, and P. E. Cladis, Electrocon-vection in nematic liquid crystals: comparison between experimental results and the hydrodynamic model, *Phys. Lett. A* **235**(5), 508–514, (1998). doi: 10.1016/S0375-9601(97)00680-4

65. T. Tóth-Katona, N. Éber, and Á. Buka, Temporal response to harmonic driving in electroconvection, *Phys. Rev. E* **83**(6), 061704/1–8, (2011). doi: 10.1103/PhysRevE.83.061704

66. M. Treiber, and L. Kramer, Bipolar electrodiffusion model for electroconvec-tion in nematics, *Mol. Cryst. Liq. Cryst.* **261**(1), 311–326, (1995). doi: 10.1080/10587259508033478

67. D. Wiant, J. T. Gleeson, N. Éber, K. Fodor-Csorba, A. Jákli, and T. Tóth-Katona, Nonstandard electroconvection in a bent-core nematic liquid crystal, *Phys. Rev. E* **72**(4), 041712/1–12, (2005). doi: 10.1103/PhysRevE.72.041712

68. S. Tanaka, S. Dhara, B. K. Sadashiva, Y. Shimbo, Y. Takanishi, F. Araoka, K. Ishikawa, and H. Takezoe, Alternating twist structures formed by electro-convection in the nematic phase of an achiral bent-core molecule, *Phys. Rev. E* **77**(4), 041708/1–5, (2008). doi: 10.1103/PhysRevE.77.041708

69. S. Tanaka, H. Takezoe, N. Éber, K. Fodor-Csorba, A. Vajda, and Á. Buka, Electroconvection in nematic mixtures of bent-core and calamitic molecules, *Phys. Rev. E* **80**(2), 021702/1–8, (2009). doi: 10.1103/PhysRevE.80.021702

70. P. Tadapatri, U. S. Hiremath, C. V. Yelamaggad, and K. S. Krishnamurthy, Patterned electroconvective states in a bent-core nematic liquid crystal, *J.*

Phys. Chem. B **114**(1), 10–21, (2010). doi: 10.1021/jp9058802

71. D. Wiant, K. Neupane, S. Sharma, J. T. Gleeson, S. Sprunt, A. Jákli, N. Pradhan, and G. Iannacchione, Observation of a possible tetrahedric phase in a bent-core liquid crystal, *Phys. Rev. E* **77**(6), 061701/1–7, (2008). doi: 10.1103/PhysRevE.77.061701

72. E. Dorjgotov, K. Fodor-Csorba, J. T. Gleeson, S. Sprunt, and A. Jákli, Viscosities of a bent-core nematic liquid crystal, *Liq. Cryst.* **35**(2), 149–155, (2008). doi: 10.1080/02678290701824199

73. C. Bailey, K. Fodor-Csorba, J. T. Gleeson, S. Sprunt, and A. Jákli, Rheological properties of bent-core liquid crystals, *Soft Matter* **5**(19), 3618–3622, (2009). doi: 10.1039/B907261F

74. M. Majumdar, P. Salamon, A. Jákli, J. T. Gleeson, and S. Sprunt, Elastic constants and orientational viscosities of a bent-core nematic liquid crystal, *Phys. Rev. E* **83**(3), 031701/1–8, (2011). doi: 10.1103/PhysRevE.83.031701

75. A. N. Trufanov, M. I. Barnik, L. M. Blinov, and V. G. Chigrinov, Electrohydrodynamic instability in homeotropically oriented layers of nematic liquid crystals, *Sov. Phys. JETP* **53**(2), 355–361, (1981) [*Zh. Eksp. Teor. Fiz.* **80**(2), 704–715, (1981)].

76. D. K. Rout, and R. N. P. Choudhary, Electrohydrodynamic instability in some nematic cyanobiphenyls in an AC electric field, *Liq. Cryst.* **4**(4), 393–398, (1989). doi: 10.1080/02678298908035485

77. E. I. Rjumtsev, and S. G. Polushin, Electrohydrodynamic instabilities in nematic liquid crystals with large positive dielectric anisotropy, *Liq. Cryst.* **13**(5), 623–628, (1993). doi: 10.1080/02678299308026335

78. L. M. Blinov, and V. G. Chigrinov, *Electro-optic Effects in Liquid Crystal Materials*. (Springer, Berlin, 1996).

79. O. D. Lavrentovich, V. G. Nazarenko, V. M. Pergamenshchik, V. V. Sergan, and V. M. Sorokin, Surface-polarization electrooptic effect in a nematic liquid crystal, *Sov. Phys. JETP.* **72**(3), 431–444, (1991) [*Zh. Eksp. Teor. Fiz.* **99**(3), 777–802 (1991)].

80. O. D. Lavrentovich, V. G. Nazarenko, V. V. Sergan, and G. Durand, Dielectric quenching of the electric polar surface instability in a nematic liquid crystal, Phys. Rev. A. **45**(10), R6969–R6972, (1992). doi: 10.1103/PhysRevA.45.R6969

81. P. Kumar, J. Heuer, T. Tóth-Katona, N. Éber, and Á. Buka, Convection-roll instability in spite of a large stabilizing torque, *Phys. Rev. E* **81**(2), 020702(R)/1–4, (2010). doi: 10.1103/PhysRevE.81.020702

82. N. Éber, L. O. Palomares, P. Salamon, and Á. Buka (unpublished).

83. E. Bodenschatz, W. Pesch, and G. Ahlers, Recent developments in Rayleigh-Benard convection, *Annu. Rev. Fluid Mech.* **32**, 709–778, (2000). doi: 10.1146/annurev.fluid.32.1.709

84. Y. Marinov, J. Kosmopoulos, W. Weissflog, A. G. Petrov, and D. J. Photinos, Flexoelectricity of wedge-like molecules in nematic mixtures, *Mol. Cryst. Liq. Cryst.* **357**(1), 221–228, (2001). doi: 10.1080/10587250108028255

85. N. Scaramuzza, and M. C. Pagnotta, Evidence for flexoelectric effect in pallated metallorganic liquid crystals, *Mol. Cryst. Liq. Cryst.* **239**(1), 263–267,

(1994). doi: 10.1080/10587259408047188

86. L. K. Vistin', I. G. Chistyakov, R. I. Zharenov, and S. S. Yakovenko, Changes in the domain pattern of nematic liquid crystals in electric fields, *Sov. Phys. Crystallogr.* **21**(1), 91–93, (1976) [*Kristallografiya* **21**(1), 173–177, (1976)].

87. T. Takahashi, S. Hashidate, and T. Akahane, Novel measurement method for flexoelectric coefficients of nematic liquid crystals, *Jpn. J. Appl. Phys.* **37**(4A), 1865–1869, (1998). doi: 10.1143/JJAP.37.1865

88. Y. Marinov, A. G. Petrov, and H. P. Hinov, On a simple way for obtaining important material constants of a nematic liquid crystal: longitudinal flexo-electric domains under the joint action of DC and AC voltages, *Mol. Cryst. Liq. Cryst.* **449**(1), 33–45, (2006). doi: 10.1080/15421400600580188

89. K. Van Le, F. Araoka, K. Fodor-Csorba, K. Ishikawa, and H. Takezoe, Flex-oelectric effect in a bent-core mesogen, *Liq. Cryst.* **36**(10-11), 1119–1124, (2009). doi: 10.1080/02678290902854086

90. P. Kumar, Y. G. Marinov, H. P. Hinov, U. S. Hiremath, C. V. Yelamaggad, K. S. Krishnamurthy, and A. G. Petrov, *J. Phys. Chem. B.* **113**(27), 9168–9174, (2009). doi: 10.1021/jp903241z

91. E. Plaut, W. Decker, A. G. Rossberg, L. Kramer, and W. Pesch, New symme-try breaking in nonlinear electroconvection of nematic liquid crystals, *Phys. Rev. Lett.* **79**(12), 2367–2370, (1997). doi: 10.1103/PhysRevLett.79.2367

92. M. Oh-e, K. Kondo, and Y. Kando, Theoretical consideration of the drop in threshold voltage at low frequencies in nematic liquid crystals, *Liq. Cryst.* **17**(1), 95–107, (1994). doi: 10.1080/02678299408036551

93. H. Seiberle, and M. Schadt, LC-conductivity and cell parameters; their in-fluence on twisted nematic and supertwisted nematic liquid crystal displays, *Mol. Cryst. Liq. Cryst.* **239**(1), 229–244, (1994).
doi: 10.1080/10587259408047185